THE ASTROPHYSICAL JOURNAL, 229:533–544, 1979 April 15

H I SHELLS AND SUPERSHELLS

CARL HEILES
Astronomy Department, University of California, Berkeley
Received 1978 August 7; accepted 1978 November 1

ABSTRACT

We present photographs of H I antenna temperatures in narrow velocity intervals versus galactic longitude and latitude, for the range $10° \leq l \leq 250°$, $|b| \leq 10°$, derived from the Weaver and Williams survey. These photographs exhibit much filamentary structure. One has the impression that, if only the angular resolution were somewhat better, filamentary structure would appear even more prominently. Many of the filaments form portions of circular arcs. Some of these arcs change size with velocity in the manner expected for an expanding shell. In nearly all cases of such expanding shells only one hemisphere, either the approaching or the receding one, is apparent. The properties of 63 shells have been measured and tabulated.

The H I shells do not seem to be significantly correlated with any other types of astronomical object, except perhaps young stellar clusters. Shells range up to 1.2 kpc in radius, $2 \times 10^7\ M_\odot$ in mass, and 10^{53} ergs in kinetic energy. Their shapes tend to be circular, with a slight preference for elongation along the galactic plane. If the shells are produced by the injection of energy E_E into the interstellar medium by a sudden explosion such as a supernova, the required values of E_E range up to 6×10^{53} ergs. This energy is hundreds of times larger than that available from a single supernova.

Shells for which $E_E > 3 \times 10^{52}$ ergs are deemed "supershells" because of their outstandingly large sizes and energy requirements. Supershells are not correlated with extreme Population I objects. The number of observed supershells is less than 10, a number which is consistent with a production rate of only $10^{-7}\ \mathrm{yr}^{-1}$. The probability that the production agent has ever been directly observed is less than a few percent.

Subject headings: interstellar: matter — radio sources: 21 cm radiation

I. INTRODUCTION

Away from the galactic plane the interstellar H I, when viewed in the 21 cm line in narrow velocity ranges, is concentrated in arcs with typical diameters of tens of degrees. In some cases the diameters change with velocity in the manner expected for expanding shells. It is our belief that all such filamentary structures were once part of expanding shells which may have since slowed down and become stationary (Heiles 1976*a*). This observational picture is consistent with recent theoretical developments (Cox and Smith 1974; McKee and Ostriker 1977; Smith 1977) which have shown that the supernova rate is high enough that the appearance of the interstellar medium should be dominated by supernova explosions.

Some of the arcs observed away from the galactic plane are large and would be easily observable even if they were far away. For example, the shell in Eridanus discussed by Heiles (1976*a*) is centered at $b = 40°$ and has a diameter of 40°; if it were 20 times farther away, it would be centered at $b = 2.4°$ and would have a diameter of 2.4°. It would be visible in the galactic-plane survey of Weaver and Williams (1973), which used a 36′ angular resolution, if only the confusing effects of foreground and background gas could be eliminated. Fortunately, this can be done for most ranges of galactic longitude by examining the gas within narrow ranges of velocity; differential galactic rotation provides a relation between distance and velocity.

II. OBSERVATIONAL DATA

The survey of Weaver and Williams (1973) was used to generate numerical matrices of antenna temperatures versus galactic longitude and latitude. The angular ranges covered by the survey, 10° to 250° in longitude and $-10°$ to $+10°$ in latitude, were included in their entirety. The antenna temperatures for each matrix were obtained with the velocity resolution of the survey, $2\ \mathrm{km\ s^{-1}}$; the velocity separation between adjacent matrices was $4\ \mathrm{km\ s^{-1}}$. The velocity interval extending from -143 to $+141\ \mathrm{km\ s^{-1}}$ was covered, resulting in a total of 72 pictures.

These matrices were used to generate photographic representations of the antenna temperature versus longitude and latitude, using Berkeley's PDS microdensitometer in playback mode. These 72 pictures are displayed in Figure 1 (Plates 17–22). It was difficult to retain the full dynamic range of the data in the photographs. In particular, we were interested in the possibility of detecting very weak features while retaining the ability to distinguish difference among the intense features in the galactic plane. By trial and error we found that taking the square root of the temperatures before making the picture produced a contrast characteristic which was favorable for our purposes. The weakest features which can be discerned in Figure 1 have antenna temperatures of about 1 K.

The beamwidth of the telescope used in the Weaver and Williams (1973) survey was 36′. In Figure 1 the size of each spot which marks the 10° intervals in galactic longitude is 0°.5 in longitude by 0°.25 in latitude, and thus occupies about 35% of the area of the telescope beam.

III. SHELLS AND FILAMENTARY ARCS

Detailed inspection of Figure 1 reveals a multitude of structure, much of which is filamentary. In fact, one has the impression that, if only the angular resolution were somewhat better, a much larger fraction of the structure would be resolved into filaments and the structure would resemble a "cosmic bubble bath" (Brand and Zealey 1975). In many cases filaments are curved in a manner reminiscent of arcs produced by explosions, such as the Cygnus Loop seen in optical light. In some cases the diameter changes with velocity in the manner expected for an expanding shell, as has also been observed previously for some high-latitude structures (see, e.g., Heiles 1976*a*). It is surprising that any of the more distant structures are resolved: at 10 kpc distance, the angular resolution corresponds to a linear size of 100 pc. Distant structures are easily resolved only because they are so large, which seems to occur particularly in the exterior portions of the Galaxy.

TABLE 1

STATIONARY H I SHELLS

Name (1)	Δl (deg) (2)	Δb (deg) (3)	V_{min} (km s^{-1}) (4)	V_{max} (km s^{-1}) (5)	R_{gal} (kpc) (6)	D (kpc) (7)	log R_{sh} (pc) (8)	log n_0 (cm^{-3}) (9)	log M ($M_\odot$) (10)	log E_E (ergs) (11)	Conf. (12)
GS 012−02+25.......	3	4	+21	+29	7.0	3.1	2.0	+0.1	5.2	51.2	3
GS 013−03+75.......	7	8	+61	+89	3.9	6.5	2.6	−1.3	5.7	51.7	3
GS 016−06+43.......	3	6	+29	+57	6.4	3.8	2.2	−0.6	5.1	51.1	2
GS 018−04+87.......	3	3	+77	+97	4.1	6.8	2.3	−0.5	5.4	51.4	2
GS 018−02+63.......	3	2	+57	+69	4.0	7.0	2.2	−0.9	4.8	50.8	1
GS 022+03−31.......	6	4	−47	−15	...	0.5	1.3	+0.6	3.7	49.7	2
GS 024−01+63.......	4	6	+57	+69	6.0	4.7	2.3	−0.7	5.4	51.4	2
GS 029+02+41.......	4	4	+37	+45	7.4	3.2	2.0	−0.2	5.1	51.2	1
GS 030−07+91.......	6	8?	+85	+97	5.3	6.9	2.6	−1.3	5.7	51.7	3
GS 033+06−49.......	4	3	−59	−39	14.7	22.0	2.8	−0.8	6.8	52.9	1
GS 034−06+65.......	5	8	+49	+81	6.7	4.6	2.4	−0.3	6.0	52.1	2
GS 034+02+73.......	3	3	+65	+81	6.3	5.4	2.1	−0.3	5.3	51.4	1
GS 036+01−21.......	1	6	−31	−11	...	0.5	1.3	+0.3	3.4	49.7	1
GS 036+06+55.......	9	8?	+45	+65	7.2	3.9	2.5	−0.7	5.9	51.9	3
GS 046−01−15.......	3	4?	−23	−7	...	0.5	1.3	+0.1	3.2	49.0	1
GS 046−01+83.......	7	6	+77	+89	7.2	6.9	2.6	−0.9	6.0	52.0	2
GS 048−04+49.......	3	4	+45	+53	7.9	4.1	2.1	−0.2	5.2	51.3	2
GS 052−05+25.......	11	7	+21	+29	8.9	2.0	2.2	−0.7	5.0	51.0	3
GS 052+07+39.......	5	7	+17	+61	8.4	3.1	2.2	+0.2	6.0	52.1	3
GS 057+03−11.......	6	3	−15	−7	...	0.5	1.3	0.0	3.1	49.0	2
GS 063−01−03.......	2	2	−7	+1	...	0.5	1.0	+0.6	2.8	48.7	1
GS 063+04+13.......	4	4	+9	+17	...	0.5	1.3	+0.2	3.3	49.3	3
GS 066−01+35.......	6	6	+29	+41	9.1	4.1	2.3	−0.6	5.5	51.6	2
GS 067−02−37.......	7	8	−39	−35	11.7	11.1	2.9	−2.0	5.9	51.7	1
GS 081−05−37.......	12	10	−47	−27	11.5	7.5	2.9	−0.9	6.9	52.9	1
GS 087+03+19.......	7	7	+13	+25	...	0.5	1.5	+0.3	3.9	50.0	2
GS 088−04+17.......	6	6	+13	+21	...	0.5	1.5	+0.3	3.6	50.0	2
GS 089+03−51.......	6	4	−55	−47	12.4	7.5	2.5	−0.8	5.9	51.9	2
GS 090+02−115......	4	4	−123	−107	17.4	14.3	2.7	−1.5	5.7	51.7	2
GS 091−04−69.......	9	10	−83	−55	13.6	9.0	2.9	−1.0	6.8	52.8	1
GS 091+02−101......	4	3	−95	−107	16.0	12.3	2.6	−0.6	6.3	52.3	2
GS 117−07−67.......	7	8	−71	−63	13.7	6.3	2.6	−0.8	6.0	52.2	2
GS 128+01−105......	7	6	−107	−103	19.2	11.4	2.8	−1.4	6.3	52.2	2
GS 129−05−91.......	6	4	−95	−87	17.2	9.1	2.6	−1.2	5.8	51.8	2
GS 130+00+15.......	36	6	+9	+21	...	0.5	1.8	−1.0	3.5	49.5	1
GS 148−01+15.......	4	4	+13	+17	...	0.5	1.3	−0.3	2.8	48.7	2
GS 152−04−41.......	4	4	−47	−35	15.6	6.1	2.3	−0.5	5.7	51.7	2
GS 183+01+35.......	26	20?	−55	−15	...	0.5	2.0	−0.6	4.6	50.6	1
GS 200+05+23.......	7	7	+17	+29	14.6	4.8	2.4	−0.4	6.0	52.2	1
GS 203+02−11.......	4?	5	−19	−3	...	0.5	1.3	+0.8	3.8	49.9	1
GS 215+06−13.......	11	5	−19	−7	...	0.5	1.3	0.0	3.5	49.5	1
GS 223−02+35.......	19	19	+33	+37	12.8	3.5	2.8	−0.9	6.6	52.6	3
GS 228−05+47.......	7	7	+33	+61	13.4	4.5	2.4	−1.0	5.5	51.4	3
GS 239+02+11.......	4	4	+9	+13	...	0.5	1.3	+0.3	3.4	49.5	2
GS 241−04−05.......	16	13	−7	−3	...	0.5	1.8	−1.3	5.9	49.0	2
GS 242−01+11.......	6	6	+9	+13	...	0.5	1.5	+0.1	3.7	49.7	2

TABLE 2

EXPANDING H I SHELLS

Name (1)	Δl (deg) (2)	Δb (deg) (3)	$V_{\min}$ (km s^{-1}) (4)	$V_{\max}$ (km s^{-1}) (5)	$R_{\rm gal}$ (kpc) (6)	D (kpc) (7)	log $R_{\rm sh}$ (pc) (8)	log n_0 (cm^{-3}) (9)	log M ($M_{\odot}$) (10)	$V_{\rm sh}$ (km s^{-1}) (11)	log E_k (ergs) (12)	log E_E (ergs) (13)	Conf. (14)
GS 016−01+71......	3	2	+53	+73	4.3	6.3	2.1	+0.3	5.8	18	51.6	52.4	2
GS 022+01+139.....	4	3	+121	+141	2.1	9.5	2.5	−0.2	6.4	18	52.2	53.0	1
GS 029+00+133.....	5?	?	+113	+141	4.8	8.7	2.6	−0.9	6.3	20	52.2	52.6	1
GS 041+01+27......	14	12	+25	+37	8.6	2.0	2.4	+0.4	6.7	10	52.0	52.9	1
GS 057+01−33......	8	3	−35	−15	11.8	13.8	2.8	−0.5	7.0	18	52.8	53.6	1
GS 061+00+51......	3	4	+37	+53	8.7	4.8	2.2	0.0	5.7	14	51.3	52.1	1
GS 064−01−97......	11	6	−99	−75	16.1	16.9	3.1	−1.2	7.1	22	53.1	53.8	1
GS 071+06−135.....	12?	11?	−135	−119	20.7	21.6	3.3	−1.3	7.8	16	53.5	54.2	3
GS 075−01+39......	11	6	+17	+41	9.7	2.6	2.3	+0.2	6.2	22	52.2	52.9	1
GS 088+02−103.....	7	5	−119?	−79	17.0	12.6	2.8	−0.3	7.3	24	53.4	54.1	2
GS 095+04−113.....	10	5	−123	−103	17.0	12.9	2.9	−0.6	7.3	10	52.6	53.5	1
GS 103+05−137......	6?	13?	−139	−123	20.4	15.6	3.1	−1.4	7.0	14	52.6	53.4	2
GS 108−04−23......	5	11?	−39	−15	11.0	2.5	2.2	+0.4	6.1	16	51.9	52.7	1
GS 123+07−127.....	8	8	−131	−115	22.2	15.1	3.2	−1.7	7.4	12	52.9	53.3	2
GS 139−03−69......	18	10	−87	−59	16.0	7.1	3.3	−0.8	8.2	18	54.0	54.8	3
GS 224+03+75......	11	7	+61	+77	16.3	7.6	2.8	−0.5	7.0	14	52.6	53.4	2
GS 242−03+37......	15	15	+33	+57	12.1	3.6	2.7	+0.3	7.5	20	53.4	54.2	3

We have searched Figure 1 for filaments or sharp boundaries of holes which appear to be parts of closed circles or ovals, and we list their properties in Tables 1 and 2. In the remainder of this paper we call these objects "shells." Table 1 presents shells which show no change in size with velocity and contains the majority of shells. The shells in Table 2 appear to change size with velocity.

a) *Description of Tables*

Each table presents a name in column (1). The form of these names is borrowed from the traditional form for galactic objects. For example, the name of the first object in Table 1 is GS 012−02+25. GS denotes that the object is a galactic shell, 012 is the galactic longitude of the center, −02 the latitude, and +25 the LSR velocity. The method of choosing the velocity is described in § III*b*(iii). Columns (2) and (3) contain the size of the shell in longitude (Δl) and latitude (Δb), respectively. Columns (4) and (5) give the minimum and maximum velocities between which the object is visible in Figure 1. Column (6) lists the galactic radius $R_{\rm gal}$, and column (7) the distance, both in kiloparsecs. Column (8) records the radius of the object in parsecs, equal to half of the geometric mean of the sizes in columns (2) and (3). Column (10) gives the logarithm of the mass of the shell in solar masses, and column (9) the density of the ambient material before formation of the shell. In Table 1 column (11) lists the logarithm of the energy E_E which would be required to produce the shell by a sudden explosion, defined in § III*d*. Column (12) of Table 1 contains our "confidence rating" of the reality of the shell, discussed in § III*b*. Table 2 is similar. The velocity in the name is the velocity at which the shell appears to attain its maximum diameter, which should be equal to the velocity of the ambient medium before the shell started to expand. Column (11) gives the expansion velocity estimated from Figure 1, column (12) the kinetic energy of the shell, column (13) E_E, and column (14) our confidence rating.

b) *Reliability of Tables*

i) *Overall Reliability*

It is not always obvious whether a shell is simply a superposition of unrelated filaments. Even when a shell appears to be isolated and relatively well defined, the determination of its diameter is a subjective procedure. As discussed in § III*c*, masses and densities are particularly uncertain.

We include in the tables a numerical evaluation of our confidence in the reality of each object on a scale of 1 to 3, where 1 indicates high confidence. The assignment of this evaluation is itself a subjective procedure, and is based on such criteria as the number of nearby objects, the angular size of the object, the degree to which the filaments form a well-defined portion of an arc, and the intensity of the features. The sample in the tables is unsuitable for statistical purposes because an object can be discerned much more easily when the velocity gradient with distance is large in absolute value such as occurs near the tangent points in the galactic interior, or when there is little gas present such as occurs if the velocity is "forbidden" under galactic rotation.

ii) *Table 2*

In some cases it is difficult to decide whether what seems to be a change with velocity is caused simply by the presence of varying amounts of foreground or background material. In the most doubtful cases we have listed the shell in Table 1. Nevertheless, there may be reason to believe that some of the shells in Table 2 should, in fact, appear in Table 1.

Only one hemisphere of most of the shells in Table 2 is visible. The number of shells with easily visible approaching and receding hemispheres is the same.

The fact that only one hemisphere is visible is disturbing. However, this is also the case for the two best examples of large shells at high latitudes (Heiles 1976*a*; Colomb, Poppel, and Heiles 1979). A simple physical explanation invokes the nonuniform distribution of interstellar gas, or the occurrence of explosions just inside or outside of a spiral arm.

It is perhaps disturbing that 80% of the shells having negative velocity have receding (positive-velocity) shells while 80% of the shells having positive velocity have approaching shells. Consider a relatively distant negative-velocity shell located near the outer boundary of the Galaxy. At the particular longitude of the shell, antenna temperatures increase as the velocity becomes less negative owing to the presence of more gas at smaller galactic radii. A shell which, by itself, shows no change with velocity might appear to become smaller in diameter owing to the presence of unrelated gas, located at the same longitude, at more positive velocities. However, we have examined several shells in Table 2 in detail, using photographs spaced at much closer velocity intervals.

One example is shown in Figure 2, where GS 095+04−113 is shown at intervals of only 1.16 km s^{-1}. This picture shows the increase in shell diameter with velocity very clearly. We have no doubt that this shell and the few other examples examined with similar scrutiny are real. These examples bolster our confidence in the proper placement of shells in Table 2.

We recall that the velocity interval covered by each picture is only 2 km s^{-1}. Therefore, the pictures in Figure 1 do not constitute a complete sample in velocity. Changes of shell size with velocity would have been more easily discerned if we had presented a complete sampling of velocity in Figure 1. However, the author feels that the sample presented is sufficient, and the number of pictures in Figure 1 is already large.

In conclusion, we assume for the remainder of this paper that all of the objects in Table 2 do, in fact, belong there.

iii) *Estimating the Distances*

An estimate of the distance to an object in the galactic plane can be obtained from the velocity of the object and the use of a galactic rotation curve. The rotation curve is well defined in the galactic interior. But in the interior, there is the well-known ambiguity between the "near" and the "far" points of intersection of the line of sight with a circle having the object's galactic radius. In the galactic interior we have assumed each object to be located at the near point.

a) *Objects outside of the solar circle.*—The galactic rotation curve is unknown outside of the "solar circle" having the galactic radius of the Sun. It has been customary to use Schmidt's (1965) extrapolation of the rotation curve, which assumes that there is little additional mass resident outside of the solar circle. However, observations of external galaxies (e.g., Roberts 1975; review by Rubin 1978) have shown that the rotation curves remain flat for remarkably large values of the radii. One might well expect the same from our own Galaxy, and indeed there are some indications that this is the case (Knapp 1978; Rubin 1978). Thus a second possibility is to use a flat curve, which assumes that there is a great deal of mass resident outside of the solar circle. These two possibilities represent opposite extremes between which the true rotation curve almost certainly lies. Schmidt's curve provides smaller distances and galactic radii than does the flat curve. The distance of each object outside of the solar circle was computed using both curves (assuming a rotation velocity of 250 km s^{-1} and a solar radius of 10 kpc for the flat curve); the maximum ratio of the two derived distances was 1.67. Each galactic radius in the tables is the geometric mean of the radii computed from the two curves, and the distance is derived from this value of the radius. Therefore, errors arising from the uncertainty in the galactic rotation curve should be less than 35%.

b) *Uncertainties arising from velocity dispersion and streaming.*—Velocity dispersion and streaming contribute a substantial uncertainty to the derived distances and galactic radii. The most obvious characteristic visible in Figure 1 is the absence of H I in various longitude ranges, which depend on velocity. At positive velocities and $l < 90°$ we are viewing hydrogen in the interior of the Galaxy; the fuzziness of the cutoffs and the departure from smoothness in the relation between longitude and cutoff velocity are produced by the velocity dispersion of the gas in the galactic interior. At all of the other cutoffs—i.e., for positive velocities at $l < 90°$ and for both positive and negative velocities at $l > 90°$—we are viewing gas in the extreme outer reaches of the Galaxy. Here the fuzziness of the cutoffs is produced by not only the velocity dispersion of the gas but also the variation in radial extent of the gas in various directions.

We estimate the velocity dispersion by estimating the velocity range over which H I is visible near $l = 180°$. We estimate a total range of 32 km s^{-1}, i.e., ± 16 km s^{-1}. An independent test of the adequacy of this velocity range for our purposes can be obtained by considering the gas in the extreme outer reaches of the Galaxy, visible near $l = 90°$ at the highest negative velocities shown in Figure 1. If the gas moves in a circular orbit, the observed velocity V is given by

$$V = R_0(\omega_R - \omega_0) \sin l$$

(Schmidt 1965), where R is the distance from the galactic center, ω is the angular velocity, and the subscript zero denotes the Sun. For constant R, V reaches a maximum at $l = 90°$. If the gas is distributed uniformly in azimuth and orbits the Galaxy in circles, the pictures at the largest negative velocities should show a concentration of gas centered at $l = 90°$. Instead, however, the gas is centered at $l \approx 105°$ for $V = -139$ km s^{-1}, at which velocity it becomes barely visible. Gas becomes easily visible at $l = 90°$, extending to $l \approx 75°$ for $V = -127$ km s^{-1}, a discrepancy of 12 km s^{-1}.

This discrepancy can be accounted for by making one of two extreme assumptions. First, we might suppose that motions are purely circular but that there is

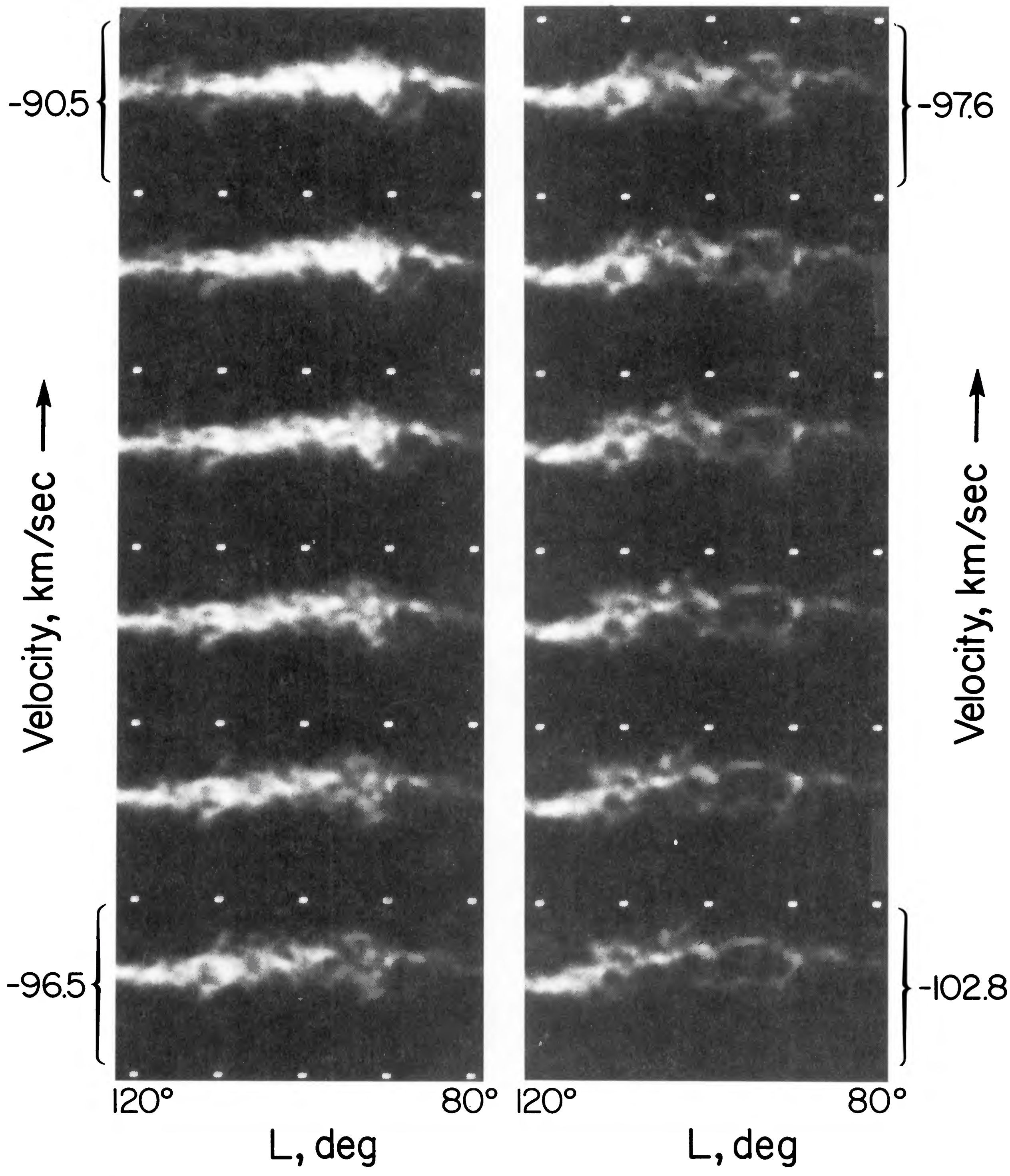

FIG. 2.—A detailed look at GS 095+04−113. Each of the twelve pictures is a photographic representation of the H I line intensity in a 2 km s^{-1} wide velocity interval, spaced 1.16 km s^{-1}. In each picture longitude increases from right to left as indicated and latitude increases from −10° at the bottom to +10° at the top. The average velocities of four of the pictures are written at their edges. The velocity of each picture is not quite constant; it varies quadratically with longitude by ±3 km s^{-1}.

a deficiency of gas in the extreme outer reaches of the galaxy at $l = 90°$, relative to $l = 105°$. Using the Schmidt (1965) rotation curve for the outer parts of the Galaxy, this would imply that the gas at $l = 105°$ extends to $R = 18.5$ kpc while the gas at $l = 90°$ extends only to 16.7 kpc. Alternatively, we might suppose the other extreme of uniform azimuthal distribution of gas. In this case, if we assume that the gas at $l = 105°$ has a purely circular orbit, the gas at $l = 90°$ has an outward radial motion of 17 km s^{-1}. The same numerical result is also obtained with the flat rotation curve defined above. Since the gas at $l = 105°$ could also have some inward radial motion, the velocity discrepancy lies within our range of ± 16 km s^{-1}.

In summary, our total range of 32 km s^{-1} appears to be representative of that part of the Galaxy with $R > R_0$. This is much larger than the observed one-dimensional dispersion of 8 km s^{-1} often adopted (see, e.g., Spitzer 1968). We will arbitrarily assume that this value is representative of the whole Galaxy. We also assume that the peculiar velocities of the objects themselves are negligible. However, as discussed below, a few objects have velocities forbidden by an amount greater than 16 km s^{-1}, which shows that our range is not large enough to encompass *all* of the departures from pure rotation.

The total uncertainty arising from velocity dispersion consists of two contributions: the 32 km s^{-1} velocity range discussed above, and the range of velocities over which an object is visible as listed in the tables. For each object two values of distance and galactic radius were calculated by using two extreme values for the velocity. One extreme is the maximum velocity in the tables plus 16 km s^{-1}; the other is the minimum velocity minus 16 km s^{-1}. For objects in Table 1 the maximum and minimum velocities are simply the velocity extremes at which the object is visible in Figure 1. For objects in Table 2 the appropriate velocities are those between which the diameter is largest, which were estimated from Figure 1. The distance and galactic radius given in the tables are the average of the values calculated for the extreme velocities.

There are a few objects which had extreme velocities which were forbidden. Distances could not be derived for these objects using the above procedure. There are two classes of forbidden velocities. The first comprises objects located at $l > 90°$ having relatively small velocities of the wrong sign. All such objects should be located near the Sun, having abnormally large peculiar velocities (perhaps arising from their motion in an expanding shell), and we have arbitrarily assumed their distances to be 500 pc; in such cases we have not entered a value for the galactic radius $R_{\rm gal}$. The second comprises objects in the galactic interior having velocities too large, for example, GS 066$-$01$+$35 in Table 1. These objects were assumed to be located at the tangent point; i.e., they were assigned the maximum galactic radius consistent with their longitude.

There is a third class of object for which distances are extremely uncertain. These are objects located at $0° < l < 90°$ and having one positive and one negative value of extreme velocity. For example, GS 063$+$04$+$13 in Table 1 has extreme velocities of -7 and 33 km s^{-1}. The negative velocity implies a distance of about 9 kpc; the positive velocity implies that the shell could be located very close to the Sun. In such cases we have not entered a value for the galactic radius and have arbitrarily assumed a distance of 500 pc.

Errors in distance affect our derived quantities in different ways, as follows: densities scale as distance^{-1}; masses as distance^2; and energies as distance^2.

c) *Hydrogen Content*

We assumed that each object in Table 1 is part of a shell which is no longer expanding. Most of these objects are weak and discernible only as a circular arc. Such a shell is brightest at the edge where the line of sight runs through the longest path length in the shell. To derive total mass, we assumed that this path length was 3 times the radial extent of the shell, and we estimated the column densities at the edge using the contour maps of Weaver and Williams (1974).

A shell which is still expanding does not exhibit large antenna temperatures near the edge and thus does not appear brighter at the edge. This occurs because the velocity width of the profiles near the edge is large owing to the expansion. To derive total mass, we estimated the column densities near the middle of the shell from Weaver and Williams (1974) and assumed that these were equal to the column density through the shell for the entire sphere. This assumption is in fact inconsistent with the typical observed situation, discussed above, that only one hemisphere of a shell is visible.

Hydrogen masses were multiplied by 1.4 to account for the presence of helium. The ambient density in the region which existed before the formation of the shell was calculated simply by dividing the total hydrogen mass by the volume of the shell.

Column densities are difficult to measure accurately because a feature is superposed on other H I in the line of sight, which has its own angular structure. This, together with the geometrical assumptions which were made, leads to low accuracies in the derived hydrogen content.

d) *Energies*

We assume that these shells are expanding, although in fact an expanding shell cannot be distinguished from a contracting one, and that they were produced by deposition of energy E_E at the center. Possible sources for such energy which have been mentioned are energetic stellar winds (Castor, McCray, and Weaver 1975; Weaver, McCray, and Castor 1977) and, of course, supernovae. In the current discussion we assume that the deposition of energy was instantaneous, as would be produced by a supernova; only the numerical details would be affected if the energy deposition were to occur over longer time intervals, as would happen with stellar winds.

During the late stages of an explosion, when the mass of interstellar gas participating in the expansion is much greater than the mass originally ejected by the explosion itself, there are three important phases. The first is the adiabatic (Sedov 1959) phase, characterized by negligible energy loss to radiation. During this phase the total energy, consisting of thermal energy and mass motion, is constant and the fraction of energy which resides in the two components remains constant. In this case

$$E_E = 1.3 \times 10^{42} n_0 R^3 V^2 \tag{1}$$

(Cox 1972), where E_E is the total energy deposited, R is the radius of the shock front, and n_0 is the ambient density (in cm^{-3}). Note that $E_E \propto MV^2$, where M is the total mass which was originally resident within radius R. Our shells cannot be in the Sedov phase; the fact that we see H I proves that much energy has been lost to radiation. The next phase is the expanding shell phase, in which a cool shell of material expands somewhat faster than at constant momentum. Numerical fits (Chevalier 1974) show that, during this phase,

$$E_E = 5.3 \times 10^{+43} n_0^{1.12} R^{3.12} V_{\text{sh}}^{1.4} . \tag{2}$$

V_{sh} is the velocity of the shell (in kilometers per second). This is the equation appropriate to objects in Table 2, which are observed to be expanding.

The numerical coefficient in equation (2) depends on the radiative energy-loss rate L and thus on the heavy-element abundance. The heavy-element abundance decreases with galactic radius, both for our own and for external galaxies (see reviews by Peimbert 1975, 1978), probably by more than an order of magnitude over the range of galactic radii encountered in Tables 1 and 2. Cox (1972), in his approximate analytical treatment, finds that the time of onset of the expanding shell phase varies as $L^{-5/11}$. This implies that, in equation (2), $E_E \propto L^{-0.19}$. This is a relatively weak dependence, reducing E_E by only 50% for a factor of 10 increase in heavy-element abundance; we shall neglect this variation in the ensuing discussion.

The final phase occurs when the velocity of the shell has become comparable to the random velocity of other shells, or of interstellar clouds. One relation can be obtained by setting V_{sh} in equation (2) equal to the one-dimensional rms velocity of interstellar clouds, 8 km s^{-1} (Spitzer 1968); this is smaller than the total rms cloud velocity of 14 km s^{-1} which is obtained by assuming the velocity distribution to be isotropic and may represent an underestimate of the required energy. We obtain

$$E_E = 9.7 \times 10^{44} n_0^{1.12} R^{3.12} . \tag{3}$$

Another relation can be obtained by setting the pressure of the hot gas inside the shell, which decreases nearly adiabatically as the gas expands, equal to the ambient pressure which characterizes the interstellar medium; we have

$$E_E = 3.6 \times 10^{45} n_0^{0.5} R^{3.12} P_{04}^{0.62} \tag{4}$$

(McKee and Ostriker 1977). Here P_{04} is the ambient pressure divided by Boltzmann's constant (units: 10^4 cm^{-3} K). A reasonable choice for P_{04} is 0.125, which is smaller than values generally considered applicable to the solar neighborhood; this value characterizes the galactic corona and should be the minimum value throughout the Galaxy in the McKee and Ostriker (1977) theory of the interstellar medium regulated by supernova outbursts. This minimum value of P_{04} should provide lower limits for E_E. We do not know whether equation (3) or equation (4) is more realistic, but we use the results from equation (3) for two reasons. First, equation (3) produces lower energies than equation (4); some of our derived energies are extraordinarily high, and since we cannot derive accurate results, we wish to err on the "conservative" side. This can be seen by noting that, with our choice for P_{04}, the two equations provide identical results for $n_0 = 1$ cm^{-3}; equation (3) depends more sensitively on density than does equation (4), and most of the objects have $n < 1$ cm^{-3}. Note that our values of E_E in Table 1 are lower than the values which would be obtained from equation (4), which are themselves lower limits because of our choice of P_{04}. Second, application of equation (4) to the objects in Table 2, assuming that they have zero expansion velocity, often results in E_E values greater than those obtained from use of equation (2). This is clearly unacceptable because equation (4) will be applicable to those objects only after they have expanded to even larger values of R than are listed in Table 2, and it will then provide even larger values for E_E. The reason for this apparently contradictory situation is that, with our choice of $P_{04} = 0.125$, the ambient temperature becomes so high for low ambient densities that the shell velocity is smaller than the thermal velocity of the ambient gas. In this case no shock front would be produced and the shell would no longer act as a self-contained unit moving supersonically.

Equation (4) has the advantage that the derived E_E is insensitive to the density; as mentioned in § III*c*, it is very difficult to derive accurate values of hydrogen content. Some of our derived densities are very low, particularly for the more energetic shells which have large radii. Our derived densities could be too small if, for example, gas in the shell has been moved to very high z distances, as is expected to happen if the z extent of the ambient gas is relatively small, if some of the gas in the shell remains ionized, or if the gas resides in small filaments which are optically thick in the 21 cm line. If the true densities were larger than those given in the tables, the E_E values derived from equation (3) would rise accordingly; in this case the "conservative" approach would be to use equation (4). We conclude that there is a distinct possibility that the E_E values given in both Tables 1 and 2 are *underestimates.*

IV. DISCUSSION

a) *Comparison with Other Objects*

Three H I shells located near the galactic plane have been previously discovered. GS 061−0+51 was discovered by Katgert (1969); our estimates of hydrogen content are about 60% of his, which we consider good agreement. The shell around HB 21 discovered by Assousa and Erkes (1973) appears to be part of our much larger GS 087+03+19 and is a good illustration of the possible effects of confusion. Their shell is 2°.7 in diameter, while GS 087+03+19 is 7° in diameter; definitive study of this region requires high-resolution observations over a large area. The W44 shell of Knapp and Kerr (1974) is not visible at all in Figure 1, possibly because its diameter is only 1°, somewhat less than twice the angular resolution of the data in Figure 1.

The catalogs of radio-continuum–emitting supernova remnants (SNRs) by Milne (1970), Downes (1971), Ilovaisky and Lequeux (1972*a*), Green (1974), and Clark and Caswell (1976) contain 16 remnants having diameters 1° or larger, and Figure 1 was examined for the presence of coincident H I shells. We found only some faint H I features not listed in Tables 1 and 2 which might possibly be associated with these SNRs. These are the following: an H I hole, 2° diameter, visible from -95 to -79 km s^{-1}, centered near G82.2+5.4 (diameter 1°.3); an arc-shaped H I filament, perhaps 9° diameter, visible from -95 to -67 km s^{-1}, centered near HB 21 (G98.1+4.7, diameter 1°.8); part of an H I shell protruding from GS 090+02−115, visible from -111 to -99 km s^{-1}, centered near G93.6−0.2 (diameter 1°); an H I hole, 2° diameter, visible from -91 to -83 km s^{-1}, centered near HB 3 (G132.4+2.2, diameter 1°.3); a possible H I hole, 2° diameter, visible at -47 km s^{-1}, centered near G156.4−1.2 (diameter 3°.2). Note that all of the H I features have high velocities and are therefore quite far away. Large-diameter radio-emitting SNRs are thought to be nearby. Unless the radio sources are not standard SNRs or the H I velocities are highly noncircular, these apparent associations must be accidental.

A further effort used maps of the radio continuum emission in the galactic plane at 408 MHz, made with angular resolution comparable to that used in the H I survey, which have been published by Haslam, Quigley, and Salter (1970) and Haslam *et al.* (1974). These were searched for weak radio features at the positions of our more prominent H I shells, with the thought that some weak features may have been overlooked. However, the confusing effects of foreground and the background position-variable emission make the identification of weak, extended circular features very difficult, and none of them were found.

The above radio-emitting SNRs include most of the classical optical-emitting, large-diameter SNRs such as the Cygnus Loop. None of the others (van den Bergh, Marscher, and Terzian 1973) show any correlation with H I shells in Figure 1. A new optical SNR has recently been discovered by Gull, Kirshner, and Parker (1977); it is located at $(l, b) = (65°, 6°)$ and is 3°.3 in diameter. There is a weak unlisted H I shell at this position which changes size with velocity, visible from -19 to -7 km s^{-1}; its diameter is 4° at -7 km s^{-1}.

The absence of any association between the H I shells and radio continuum emission is not unexpected. The Eridanus shell (Heiles 1976*a*), which is one of the two most prominent local shells, exhibits no radio continuum emission. Furthermore, Ilovaisky and Lequeux (1972*a*) show that there are fewer radio-emitting SNRs with radii larger than 15 pc than expected, and ascribe the difference to the difficulty of detecting remnants of low surface brightness. All of the shells in our tables having well-determined distances are much larger than 15 pc in radius; their radio continuum emission will be extremely difficult to detect if they follow the usual surface brightness–diameter relationship.

A search for correlations with the weak H II regions and rings in the photographic survey of Sivan (1974) revealed only one, GS 203+02−11. A search for correlations of both position and velocity of H II regions from the radio recombination line survey of Reifenstein *et al.* (1970) with features in Figure 1 yielded no positive results. Some correlations of questionable statistical significance were found with the loop structures listed by Brand and Zealey (1975). Their Hα loops Cyg 1, 2, and 3 all lie inside GS 075−01+35, and three others show possible correlations with H I shells.

A search for correlations of nearby stellar associations and galactic clusters (Becker and Fenkart 1971) with H I features, weak or strong, visible in Figure 1 yielded six positive results, as follows: III Cep (l, b, distance) = (111°, 3°, 1.0 kpc) with a small loop visible from $+5$ to $+21$ km s^{-1} which connects to GS 130+00+15; I Per (135°, −4°, 2.3 kpc) with unlisted 5° diameter shell visible from -31 to -23 km s^{-1}; NGC 1444 (148°, −1°, 1.0 kpc) with GS 148−01+15; NGC 2129 (187°, 0°, 2.1 kpc) with unlisted 3° diameter shell visible at $+21$ km s^{-1}; NGC 7092 (92°, −2°, 0.3 kpc) with unlisted 4° diameter shell visible from -23 to -3 km s^{-1}; II Mon (203°, 2°, 0.7 kpc) with GS 203+02−11. The associations and clusters which correlate with the H I shells are young; all but one have turnoff points at B1 or earlier. A physical explanation for this possible correlation involves energetic stellar winds from OB supergiant stars. As an example, the youngest star in II Mon is S Mon (= 15 Mon), an O7 $V((f))$ star studied in the UV by Snow and Morton (1976), who found that material is being ejected with velocities ranging to more than 3000 km s^{-1}. Studies in the visible by Hutchings (1976) show that the total mass loss is about 10^{-7} $M_{\odot}$ yr^{-1}. The theory of Castor *et al.* then implies that for the adopted radius of 20 pc the expansion has been occurring for the past 2×10^6 yr and that the present expansion velocity should be about 5 km s^{-1}; these numbers seem quite reasonable.

A great many more associations and galactic clusters do *not* correlate with the H I shells. Most of these have turnoff points later than B1. A diligent search, conducted with a willingness to stretch the imagination, yielded nine possible correlations with H I features out of 18 additional clusters B1 or earlier. Thus, from a total of 24 clusters, 15 show possible correlation with H I shells. This suggests that the correlation is meaningful. However, a search for correlations of H I shells with the O and B stars studied by Snow and Morton (1976), and of the stars found to have high mass-loss rates in Table 4 of Hutchings (1976), revealed only one positive result out of this sample of a dozen or so stars: HD 108 is centered on an unlisted H I shell, 3° diameter, visible from -47 to -27 km s^{-1}. We conclude that the statistical significance of any correlations with stars, OB associations, or galactic clusters is possibly meaningful.

b) *Numbers and Production Rates*

Shell lifetimes are limited by the rate at which interstellar clouds or other shells penetrate the boundary. Since typical cloud velocities are 10 km s^{-1}, typical lifetimes are (R/10) million yr. Since typical radii are nearly 100 pc, typical lifetimes are about 10^7 yr. Unfortunately, the total number of H I shells is limited by observational selection effects and is therefore unknown. However, if each Type II supernova explosion produces a shell and the Type II supernova rate is 1 explosion per 100 yr, some 100,000 shells should exist at any one time. Evidently, the number of objects listed in our tables is so small that our shells have no impact whatsoever on the derivation of the galactic supernova rate or on the rate of formation of any known astronomical object. Conversely, if shells are produced by supernovae, the number of shells should be astronomically large; we will be able to observe only the most prominent shells.

c) *Shapes*

Many of the objects in the tables have $\Delta l > \Delta b$. This is surprising because an expanding shell should decelerate less rapidly in the z direction owing to the decrease in interstellar gas density with z (Chevalier and Gardner 1974).

One possible, but unlikely, explanation is that differential galactic rotation lengthens the objects along the galactic plane. An idea of the effects of galactic rotation can be obtained by considering the evolution of the shape of a stationary, spherical shell of gas. The portion of the shell located toward the galactic interior rotates faster, producing an oval-shaped shell whose long axis is tilted, with the inside end leading the outside end. For the case of a stationary, spherical shell of gas the angle of tilt is 45° after a time $T = R_{\rm gal}/V$, where we have assumed a flat rotation curve with rotation velocity V and $R_{\rm gal}$ is the galactic radius of the center of the shell; at this time the long axis has increased to 1.5 times the original diameter and the short axis has decreased to 0.5 of the original diameter. If the diameter of the shell in the z direction remains constant, Δl can appear either longer or smaller than Δb; $\Delta l < \Delta b$ can occur only for $l > 200°$. Most of our objects have $l < 200°$ so that the tendency to be elongated along the galactic plane could, in principle, be explained by galactic rotation. However, significant elongation occurs only in times of order $R_{\rm gal}/V$, which is typically 5×10^7 yr or longer. This is a very long time, longer than or at least comparable to the expected lifetimes of a large static shell (see § IV*b*). By the time a remnant attains a significant degree of elongation, it will no longer be discernible.

A possible alternative explanation of the shapes could involve the galactic magnetic field. Observations of the field in the solar vicinity indicate that, on the average, it lies parallel to the galactic plane (see review by Heiles 1976*b*); this is the expected geometry resulting from differential galactic rotation. If $P_{04} = 0.125$, the magnetic energy density dominates if $B \geq 2$ microgauss. A general field of this strength is found from observations of Faraday rotation near the Sun and could well characterize large portions of the Galaxy. Before accepting this explanation, however, one should understand the effect of a magnetic field theoretically. Furthermore, it would be highly desirable to obtain some direct measurements of the field strength in other portions of the Galaxy, particularly the exterior portions where the interstellar density becomes small.

d) *Supershells*

Figure 3 shows the distribution of radii, H I masses, and derived values of E_E of objects for which our confidence rating is 1 and for which both extreme velocities are of the same sign and larger than 16 km s^{-1} in absolute value, so that the distances are relatively well determined. Objects having $E_E < 3 \times 10^{52}$ ergs could have been produced by one or a small number of supernovae or perhaps stellar winds. The existence of objects having larger values of E_E is harder to explain. Eleven of these "supershells" exist in our tables.

i) *Previous Observations of Supershells*

This is not the first observational indication of supershells. Westerlund and Mathewson (1966) discovered a 1 kpc diameter ring in the Large Magellanic Cloud (LMC) which is composed of arcs of H I, nonthermal radio continuum emission, and bright blue stars. More distant external galaxies have also exhibited large rings. The most spectacular are those so very prominent in the beautiful photograph of the H I

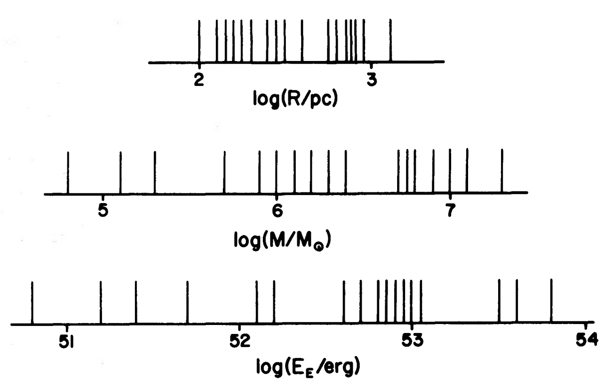

FIG. 3.—Distributions of radii, H I masses, and derived values of E_E (eqs. [2] and [3]) for shells having confidence ratings of 1 and well-determined distances.

distribution in M101 presented by Allen *et al.* (1978); these are similar in size to the largest of our supershells. In a previous paper on M101 Allen, Goss, and van Woerden (1973) reported on an H I "hole" which is not so easily visible in the photograph of Allen *et al.* (1978); this hole is 500×1500 pc in size and has an H I deficiency of about 10^7 $M_\odot$. A 340 pc diameter arc of bright stars was discovered in NGC 6946 by Hodge (1967), and a number of arcs ranging in size from 100 to 5000 pc were described by Hayward (1964). Brand and Zealey (1975) have described large shells of dust in external galaxies. Even in our own Galaxy, Lindblad (1967) and Hughes and Routledge (1972) present evidence that a model consisting of an expanding ring with dimensions of 1300×560 pc fits observations of H I and OH in the solar vicinity quite well, while Rickard (1968) suspects that the interstellar gas in the Cas-Per arm, whose velocity is some 15 km s^{-1} less than expected from galactic rotation alone, exists in the form of an 800 pc radius ring produced by an explosion which released some 10^{53} ergs.

The supershells which have been discovered in external galaxies, referenced above, are all located in the Magellanic Clouds or in the bright, blue portions of spiral galaxies. This distribution suggests that supershells are associated with Population I objects. However, the distribution of our galactic supershells is different. Only three lie inside the solar circle where our own Galaxy would appear optically bright and blue. The three objects of largest E_E, above 10^{53} ergs, all lie outside of the solar circle and have galactic radii of over 12 kpc; these largest supershells would probably be easily detectable no matter what their location in the Galaxy because they are so large. This suggests that our supershells are not associated with extreme Population I objects, which tend to be concentrated between $R_{gal} \approx 4$–8 kpc (Burton 1976), or with radio-continuum–emitting SNRs, which tend to be concentrated at $R_{gal} < 12$ kpc (Ilovaisky and Lequeux 1972*b*).

The tendency for supershells in external galaxies to be located at R_{gal} smaller than those in our own Galaxy may arise from selection effects. Many of the supershells in external galaxies were discovered optically and would tend to be located in the interior portions where the galaxies are brighter. This selection effect could be overcome by examining high-resolution high-sensitivity H I maps of external galaxies.

ii) *Possible Production Agents*

A shell which is no longer expanding will eventually be disrupted by interstellar clouds or other shells which penetrate its boundary, which happens after about 10^8 yr for supershells (see § IV*b*). The number of supershells in a given galaxy is small; there are only a handful in our own Galaxy, and a similar number in M101 and perhaps some of the other external galaxies. Supershells are therefore produced infrequently, at average intervals of perhaps 10^7 yr.

The most energetic of our supershells required nearly 10^{54} ergs if the energy was suddenly injected into the interstellar medium. This is a great deal of energy, far above the accepted values for Type II supernovae, which are about 10^{51} ergs (Woltjer 1974).

One possibility for the production of large amounts of energy is, simply, multiple supernovae. Two weak arguments favor this possibility. First, the number of galaxies observed to exhibit more than two supernovae is larger than expected on the basis of random chance (Zwicky 1974). However, in no case do those multiple supernovae occur at the same position. Second, the initial mass function varies (see, e.g., Mezger and Smith 1977; Smith, Biermann, and Mezger 1978) and in OB associations favors more massive stars to a significant degree (Blaauw 1964). Reeves (1978) has carefully considered the available evidence and finds that a typical OB association forms some 28 stars of spectral type B0 or earlier. There must be some cosmic dispersion about this grand average, with some associations forming many more such stars. The H II region W51 is probably a good example of the larger of such associations, requiring 54 O5 stars (Balick 1972) to keep it ionized. We need hundreds of such stars to produce the most energetic supershells. The most extreme OB associations might possibly have enough stars. Nevertheless, our most energetic supershells lie at large galactic radii, far from where the giant H II regions are observed (see Smith, Biermann, and Mezger 1978), which argues against this possibility.

A second, apparently unlikely possibility involves "Type III" supernovae. Zwicky's (1964) report of unpublished work by Greenstein states that this type of supernova has an expansion velocity of about 12,000 km s^{-1} with a very optically thick shell, implying an ejected mass of hundreds of solar masses; this amounts to a kinetic energy of over 10^{53} ergs, just in the required range. But in a later review, Zwicky (1965) does not stress the large kinetic energy. He also hints that Type III may be just a variant of Type II supernovae, a point made again in the review by Oke and Searle (1974). It is unfortunate that only two Type III supernovae are present in the master list of Sargent, Searle, and Kowal (1974) and that the detailed study of supernovae does not seem to command high priority at present.

It is highly unlikely that we would have seen the agent which produces a supershell. As discussed above, supershells are produced at average intervals of perhaps 10^7 yr. Surveys of external galaxies for supernovae have been in progress for about 40 yr (see, e.g., Zwicky 1974). During this time interval approximately 250,000 galaxies would have had to be searched to accumulate a reasonable probability for seeing such an infrequent event. The Palomar Supernova Search encompasses only 3003 galaxies (Sargent *et al.*), and other groups increase this number by a modest amount (see Cosmovici 1974). Thus the probability that we would have seen the agent is at most a few percent.

V. CONCLUDING REMARKS

The 36′ angular resolution of the Weaver and Williams (1973) H I survey resolves a surprising amount of detail, even at large distances. This occurs because many of the H I structures are large in linear extent and were probably produced by large amounts of energy injected directly into the interstellar medium. Nevertheless, the study of the structures would be greatly facilitated by a new survey covering the region $|b| < 10°$, having much better angular resolution. The largest available telescopes provide 10′ resolution, which would undoubtedly clarify many of the structural details which are now only barely resolved. Indications from the present data are that the structures would be for the most part filamentary in character when examined in narrow velocity intervals. Study of a larger number of these would clarify their origin and in particular should enable us to definitively confirm or deny the author's impression (Heiles 1976*a*) that all filaments are, or were, parts of expanding shells. As briefly summarized in § I, the presence of a great many interstellar shells is consistent with the recent realization of the importance of supernovae on the structure of the interstellar medium.

Supershells are a new class of object. Although they might conceivably be formed by the explosions of a large number of Type II supernovae, their lack of association with extreme Population I objects argues strongly against this possibility. Their production rate is so low that it is extremely improbable that we have ever directly observed the agent responsible for their existence. This agent may itself be a new unknown kind of astronomical object.

In order to observe the production agent directly, we will have to greatly expand the present supernova search programs. Supernova search programs and extensive H I surveys are both large, tedious projects which usually provide modest scientific return for the investment of a great deal of effort. In the present day there are many research areas which seem to provide better returns. We hope that some astronomers will nevertheless pursue these difficult programs in the future.

It is a pleasure to thank H. Weaver and A. Setteducati for the H I survey data and C. McKee for discussions about the evolution of SNRs. This work was supported in part by the National Science Foundation.

REFERENCES

Allen, R. J., Goss, W. M., and van Woerden, H. 1973, *Astr. Ap.*, **29**, 447.
Allen, R. J., van der Hulst, J. M., Goss, W. M., and Huchtmeier, W. 1978, *Astr. Ap.*, **64**, 359.
Assousa, G. E., and Erkes, J. W. 1973, *A.J.*, **78**, 885.
Balick, B. 1972 *Ap. J.*, **176**, 353.
Becker, W., and Fenkart, R. 1971, *Astr. Ap. Suppl.*, **4**, 241.
Blaauw, A. 1964, *Ann. Rev. Astr. Ap.*, **2**, 213.
Brand, P. W. J. L., and Zealey, W. J. 1975, *Astr. Ap.*, **38**, 363.
Burton, W. B. 1976, *Ann. Rev. Astr. Ap.*, **14**, 275.
Castor, J., McCray, R., and Weaver, R. 1975, *Ap. J. (Letters)*, **200**, L107.
Chevalier, R. A. 1974, *Ap. J.*, **188**, 501.
Chevalier, R. A., and Gardner, J. 1974, *Ap. J.*, **192**, 457.
Clark, D. H., and Caswell, J. L. 1976, *M.N.R.A.S.*, **174**, 267.
Colomb, R., Poppel, W., and Heiles, C. 1979, in preparation.
Cosmovici, C. B. 1974, *Supernovae and Supernova Remnants* (Dordrecht: Reidel).
Cox, D. P. 1972, *Ap. J.*, **178**, 159.
Cox, D. P., and Smith, B. W. 1974, *Ap. J. (Letters)*, **189**, L105.
Downes, D. 1971, *A.J.*, **76**, 305.
Green, A. J. 1974, *Astr. Ap. Suppl.*, **18**, 267.
Gull, T., Kirshner, R., and Parker, R. 1977, *Ap. J. (Letters)*, **215**, L69.
Haslam, C. G. T., Quigley, M. J. S., and Salter, C. J. 1970, *M.N.R.A.S.*, **147**, 405.
Haslam, C. G. T., Wilson, W. E., Graham. D. A., and Hunt, G. C. 1974, *Astr. Ap. Suppl.*, **13**, 359.
Hayward, R. 1964, *Pub. A.S.P.*, **76**, 35.
Heiles, C. 1976*a*, *Ap. J. (Letters)*, **208**, L137.
———. 1976*b*, *Ann. Rev. Astr. Ap.*, **14**, 1.
Hodge, P. W. 1967, *Pub. A.S.P.*, **79**, 29.
Hughes, V. A., and Routledge, D. 1972, *A.J.*, **77**, 210.
Hutchings, J. B., 1976, *Ap. J.*, **203**, 438.
Ilovaisky, S. A., and Lequeux, J. 1972*a*, *Astr. Ap.*, **18**, 169.
———. 1972*b*, *Astr. Ap.*, **20**, 347.
Katgert, P. 1969, *Astr. Ap.*, **1**, 54.
Knapp, G. R. 1978, paper presented at IAU Symposium No. 84, The Large-Scale Characteristics of the Galaxy, College Park, Maryland.
Knapp, G. R., and Kerr, F. J. 1974, *Astr. Ap.*, **33**, 463.
Lindblad, P. O. 1967, *Bull. Astr. Inst. Netherlands*, **19**, 34.
McKee, C. F., and Ostriker, J. P. 1977, *Ap. J.*, **211**, 135.
Mezger, P. G., and Smith, L. F. 1977, in *Star Formation*, ed. T. de Jong and A. Maeder (Dordrecht: Reidel), p. 133.
Milne, D. K. 1970, *Australian J. Phys.*, **23**, 425.
Oke, J. B., and Searle, L. 1974, *Ann. Rev. Astr. Ap.*, **12**, 315.
Peimbert, M. 1975, *Ann. Rev. Astr. Ap.*, **13**, 113.
———. 1978, paper presented at IAU Symposium No. 84, The Large-Scale Characteristics of the Galaxy, College Park, Maryland.
Reeves, H. 1978, paper presented at the Conference on Protostars and Planets, Tucson, Arizona.
Reifenstein, E. C., Wilson, T. L., Burke, B. F., Mezger, P. G., and Altenhoff, W. J. 1970, *Astr. Ap.*, **4**, 357.
Rickard, J. J. 1968, *Ap. J.*, **152**, 1019.
Roberts, M. S. 1975, in *IAU Symposium No. 69, Dynamics of Stellar Systems*, ed. A. Hayli (Dordrecht: Reidel), p. 331.
Rubin, V. C. 1978, paper presented at IAU Symposium No. 84, The Large-Scale Characteristics of the Galaxy, College Park, Maryland.
Sargent, W. L. W., Searle, L., and Kowal, C. T. 1974, in *Supernovae and Supernova Remnants*, ed. C. B. Cosmovici (Dordrecht: Reidel), p. 33.
Schmidt, M. 1965, in *Galactic Structure*, ed. A. Blaauw and M. Schmidt (Chicago: University of Chicago Press), p. 513.
Sedov, L. I. 1959, *Similarity and Dimensional Methods in Mechanics* (New York: Academic Press).
Sivan, J. P. 1974, *Astr. Ap. Suppl.*, **16**, 163.
Smith, B. W. 1977, *Ap. J.*, **211**, 404.
Smith, L. F., Biermann, P., and Mezger, P. G. 1978, *Astr. Ap.*, **66**, 65.
Snow, T. P., Jr., and Morton, D. C. 1976, *Ap. J.*, **32**, 429.
Spitzer, L., Jr. 1968, *Diffuse Matter in Space* (New York: Wiley).
van den Bergh, S., Marscher, A. P., and Terzian, Y. 1973, *Ap. J. Suppl.*, **26**, 19.
Weaver H., and Williams, D. R. W. 1973, *Astr. Ap. Suppl.*, **8**, 1.
———. 1974, *Astr. Ap. Suppl.*, **17**, 1.
Weaver, R., McCray, R., and Castor, J. 1977, *Ap. J.*, **218**, 377.
Westerlund, B. E., and Mathewson, D. S. 1966, *M.N.R.A.S*, **131**, 371.
Woltjer, L. 1974, in *Supernovae and Supernova Remnants*, ed. C. B. Cosmovici (Dordrecht: Reidel), p. 323.
Zwicky, F. 1964, *Ann. Ap.*, **27**, 300.
———. 1965, in *Stellar Structure*, ed. L. H. Aller and D. B. McLaughlin (Chicago: University of Chicago Press), p. 367.
———. 1974, in *Supernovae and Supernova Remnants*, ed. C. B. Cosmovici (Dordrecht: Reidel), p. 1.

CARL HEILES: Astronomy Department, University of California, Berkeley, CA 94720

1979ApJ...229..533H

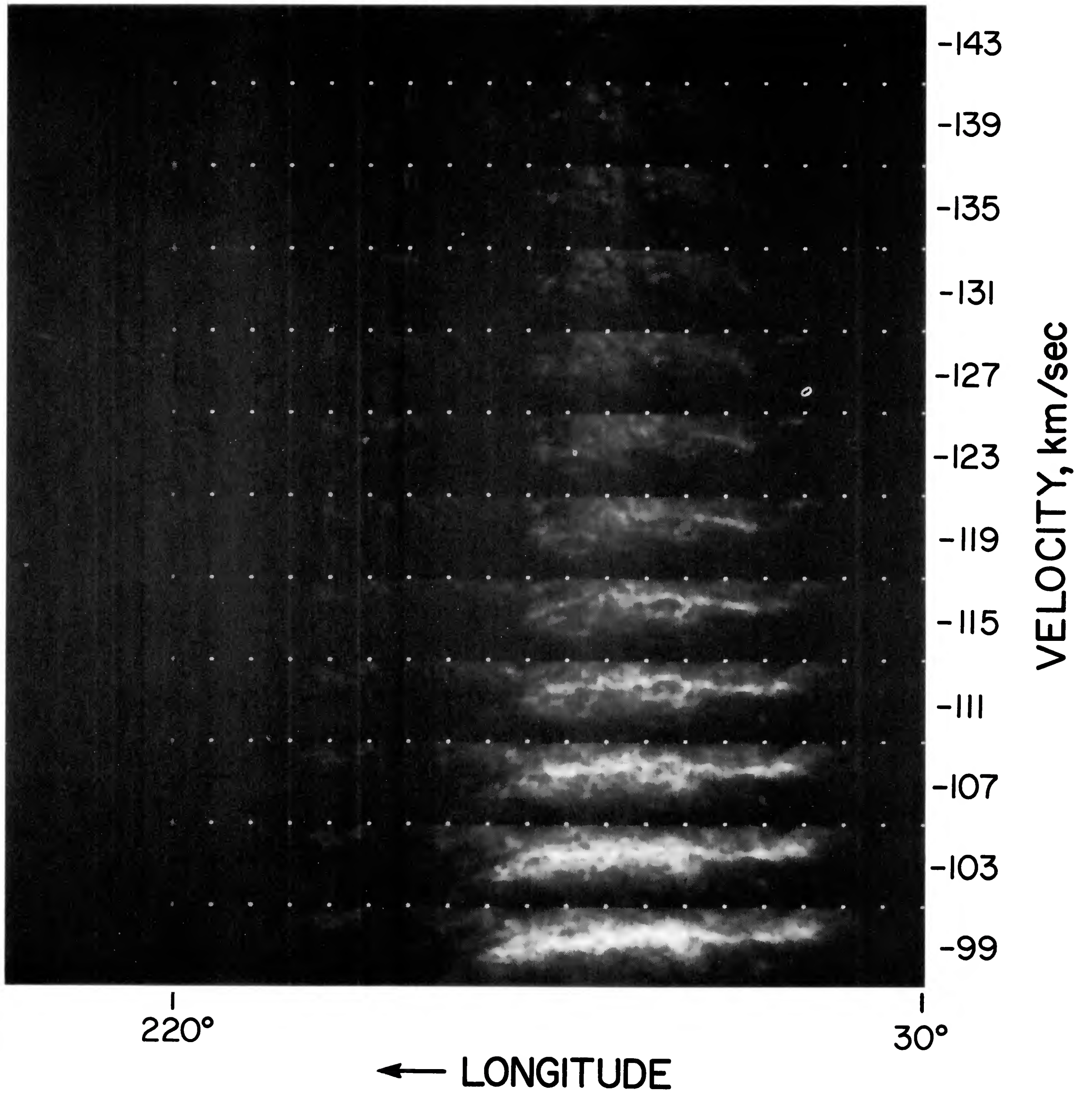

FIG. 1.—Six frames of twelve pictures each, showing a photographic representation of the H I line intensity in 2 km s^{-1} wide velocity intervals, spaced 4 km s^{-1}. In each picture longitude increases from right to left as indicated and latitude increases from $-10°$ at the bottom to $+10°$ at the top. The central velocity appears at the right-hand edge of each picture. The small white tick marks appear every 10° in longitude.

HEILES (*see* page 533)

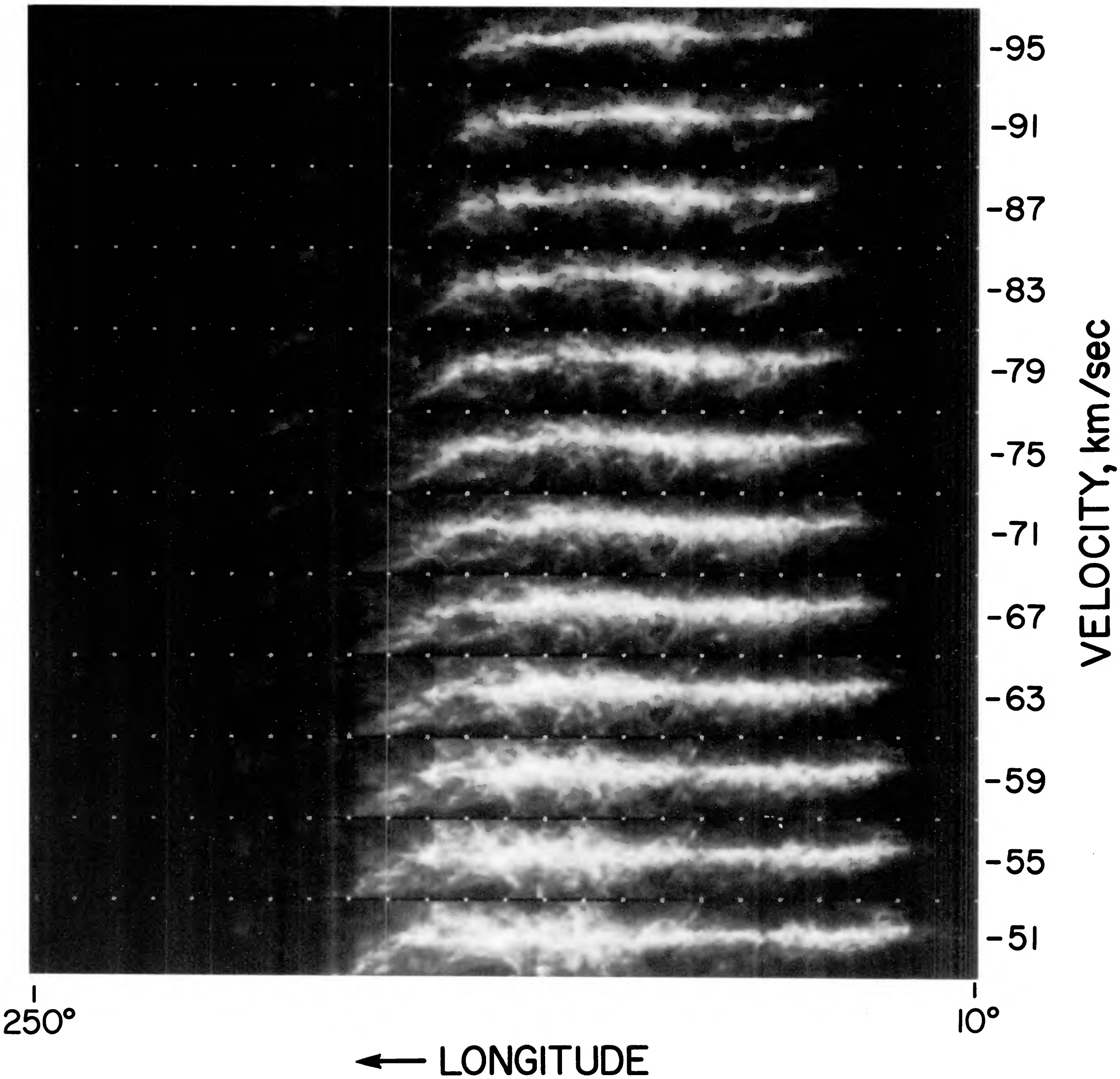

FIG. 1.—*Continued*

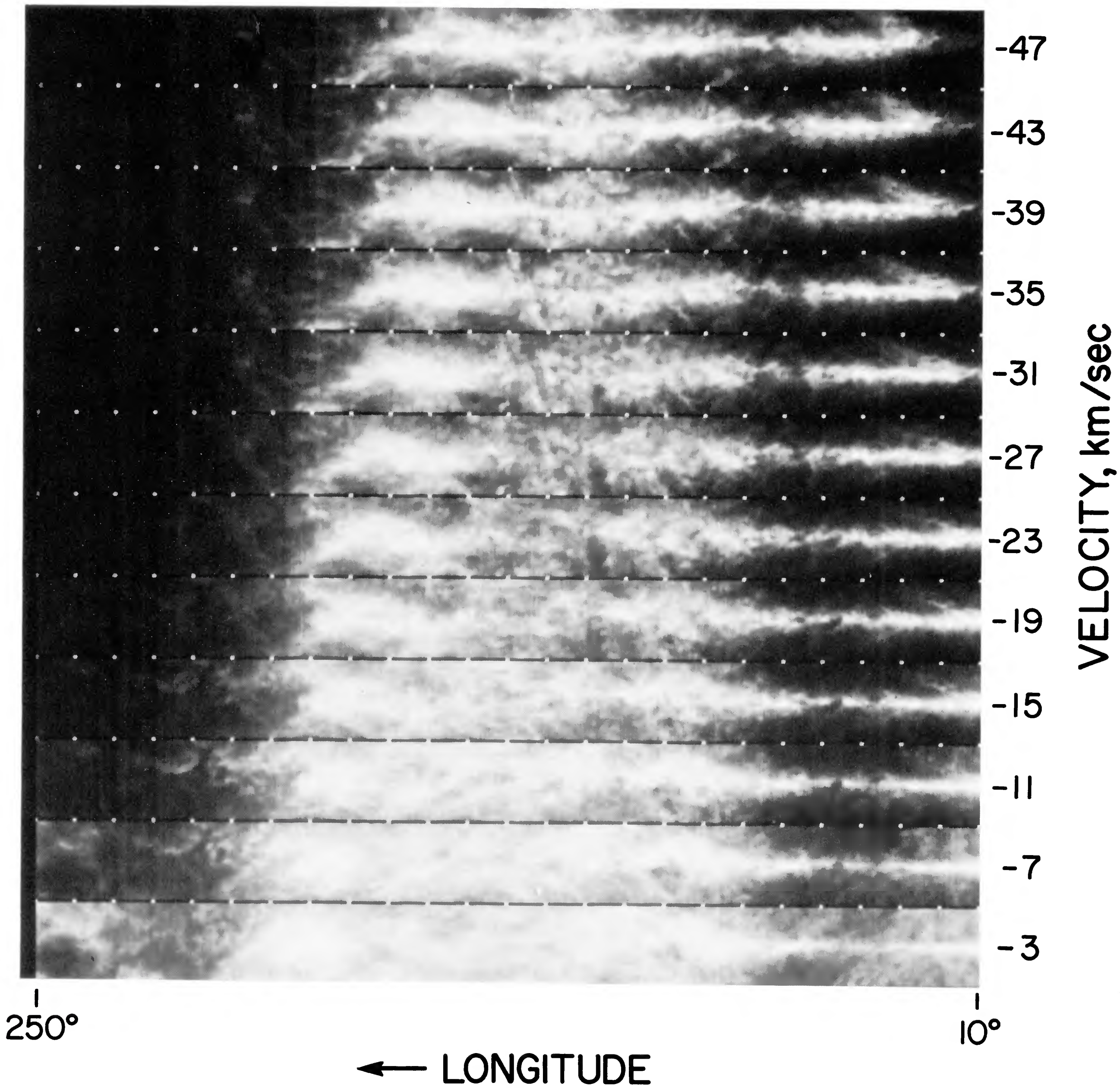

FIG. 1.—*Continued*

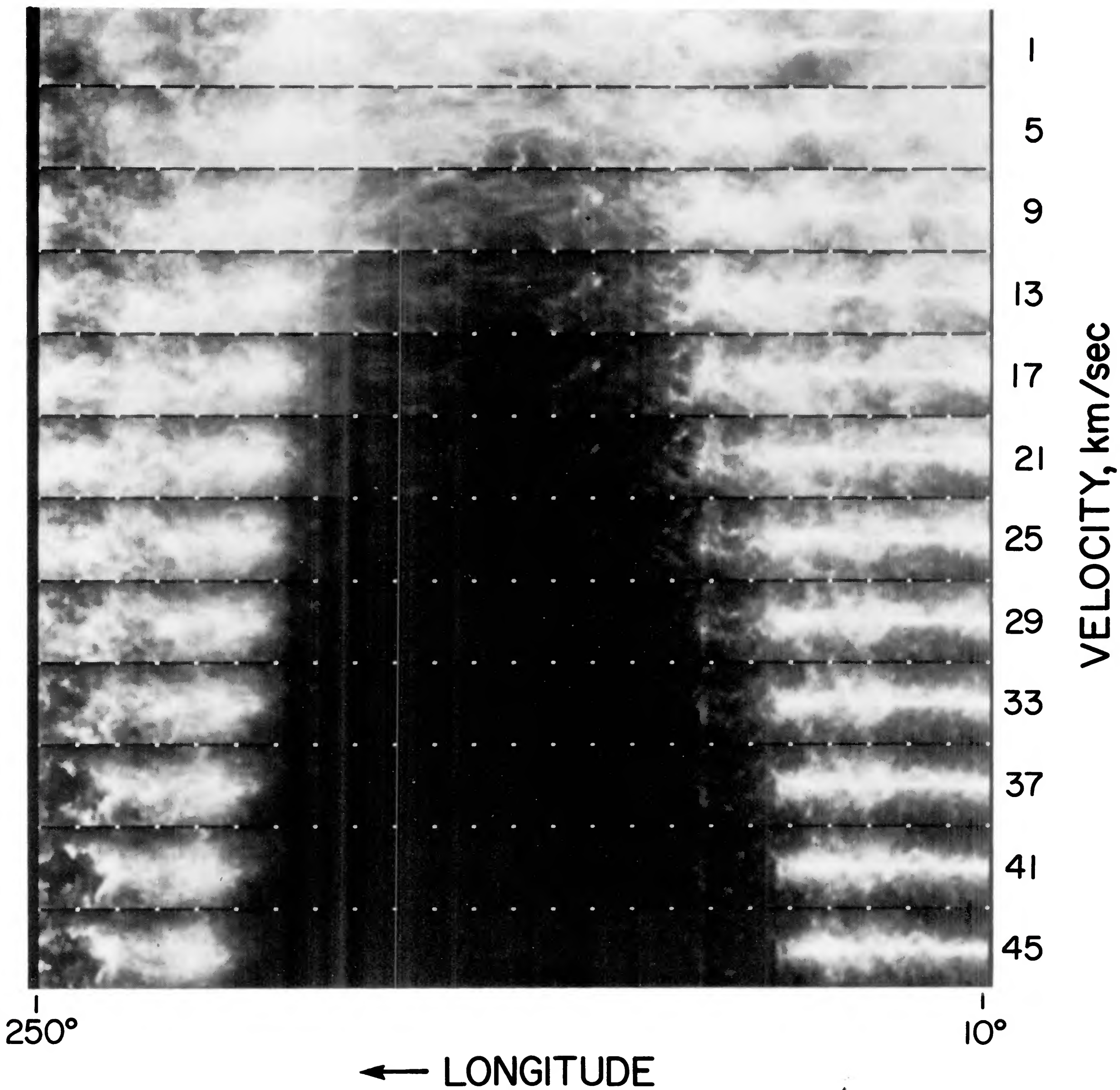

FIG. 1.—*Continued*

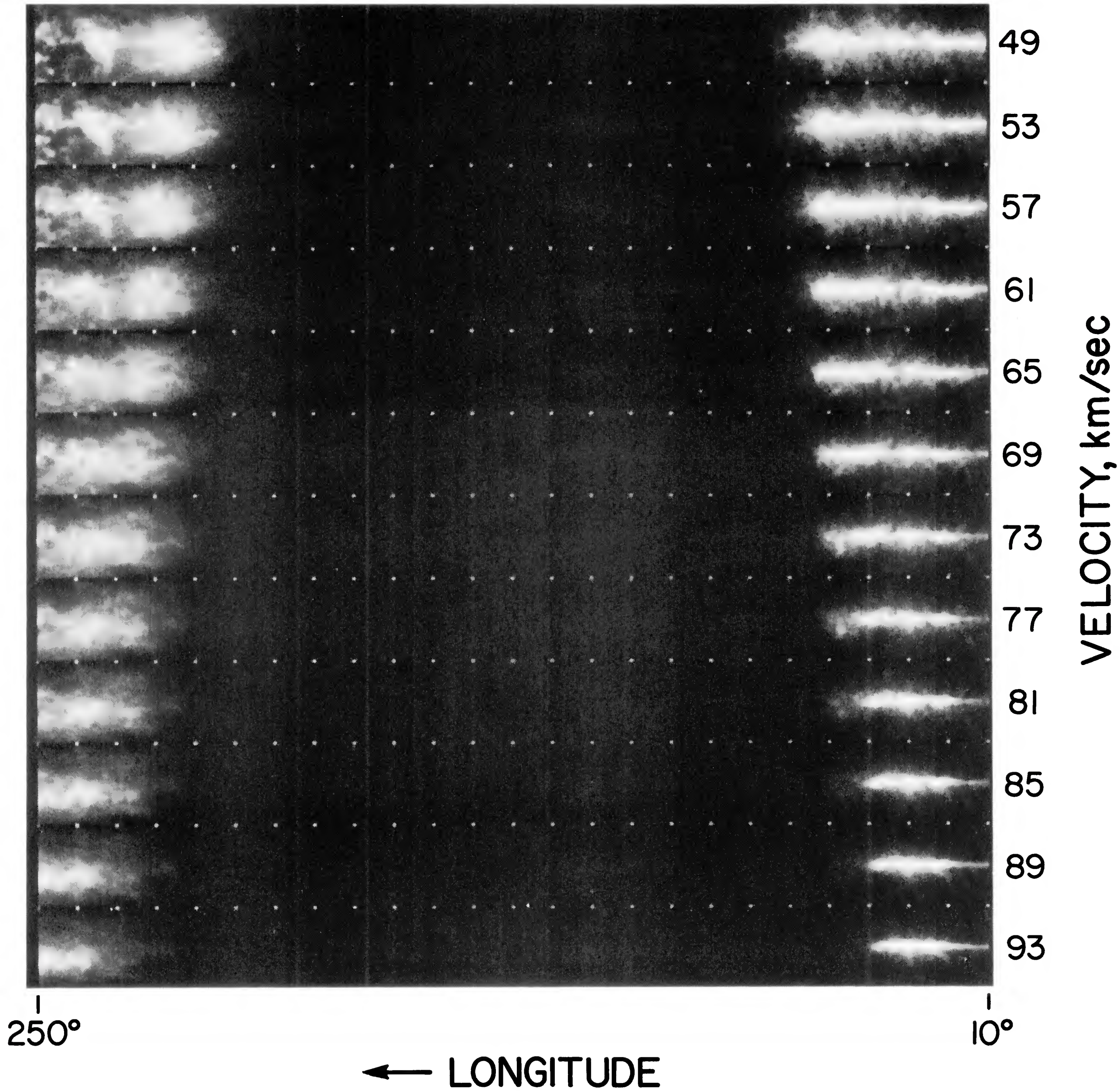

FIG. 1.—*Continued*

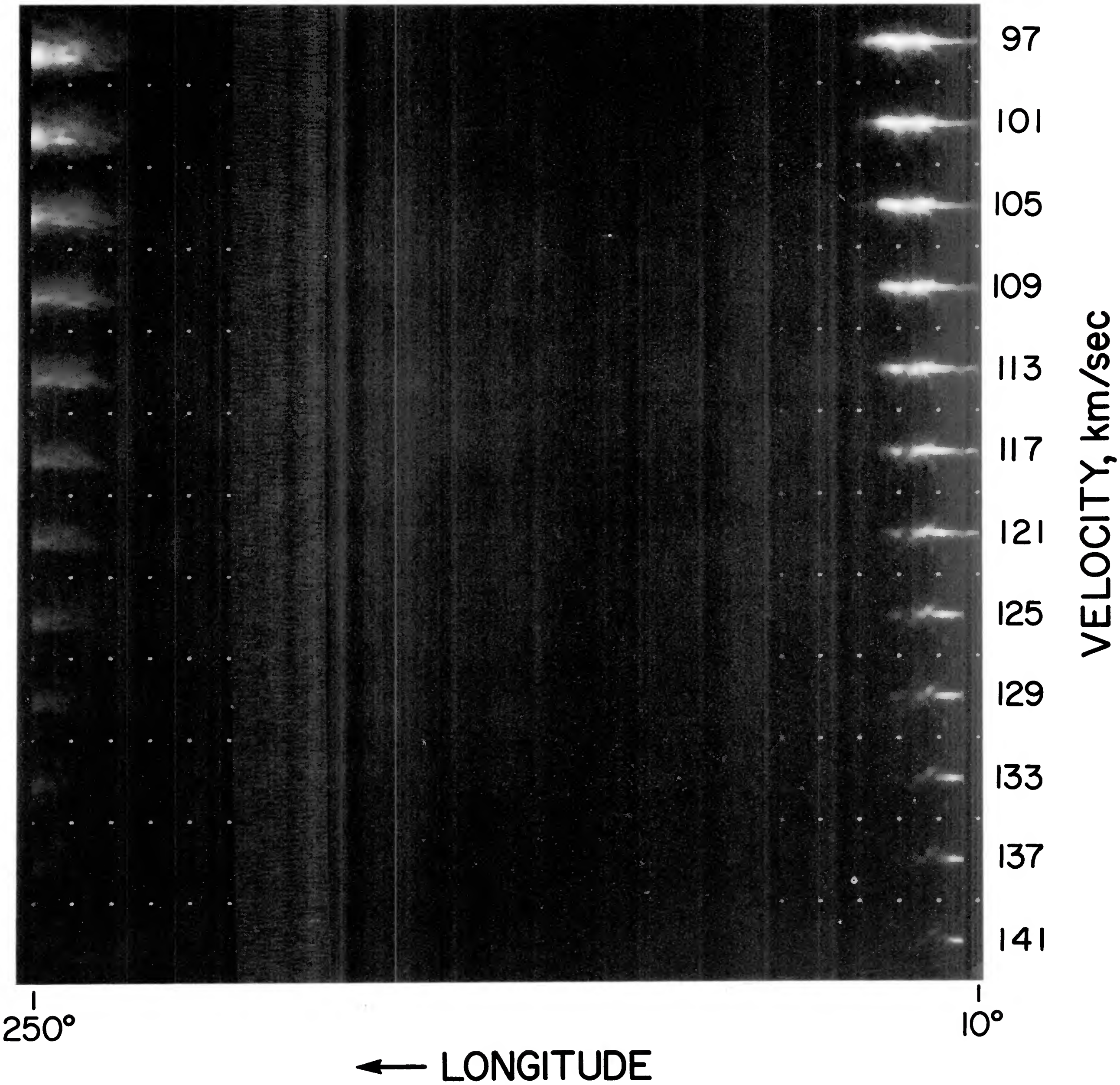

FIG. 1.—*Continued*